A novel pitch evaluation of one-dimensional gratings based on a cross-correlation filter

Xiaomei Chen[1], Ludger Koenders[2*]

[1] University of Huddersfield, Queensgate, Huddersfield HD1 3DH, United Kingdom
[2] Physikalisch-Technische Bundesanstalt (PTB), Bundesallee 100, 38116 Braunschweig, Germany
*E-mail: ludger.koenders@ptb.de

Abstract

If one-dimensional (1D), p _period and arbitrarily structured grating position-related topographical signals coexist with noise, it is difficult to evaluate the pitch practically using the centre-of-gravity (CG) method. The Fourier-transform-based (FT) method is the most precise to evaluate pitches; nevertheless it cannot give the uniformity of pitches. If a cross correlation filter −a half period of sinusoidal waveform sequence (p_T period), cross-correlates with the signals, the noise can be eliminated if $p_T \approx p$. After cross-correlation filtering, the distance between any two adjacent waveform peaks along the direction perpendicular to 1D grating lines is one pitch value. The pitch evaluation based on the cross-correlation filtering together with the detection of peaks position is described as the peak detection (PD) method in this paper. The pitch average and uniformity can be calculated by using the PD method. The computer simulation has indicated that the average of pitch deviations from the true pitch and the pitch variations are less than 0.2% and 0.2% for the sinusoidal and rectangular waveform signals with up to 50% uniform white noise, less than 0.1% and 1% for the sinusoidal and rectangular waveform signals and 0.6% and 2.5% for the triangular waveform signal if three waveform signals are mixed with Gaussian white, binomial and Bernoulli noise up to 50 % in standard deviation, one probability and trial probability respectively. As the examples, a highly oriented pyrolytic graphite (HOPG) with 0.246 nm distance between atoms and a 1D grating with 3000 nm nominal pitch are measured by a ultra-high vacuum scanning tunneling microscope (UHV STM) and a metrological atomic force microscope (AFM) respectively. After the position-related topographical signals are cross-correlation filtered, the 0.240 nm and 3004.11 nm pitches calculated by using the PD method are very close to the 0.240 nm and 3003.34 nm results evaluated by the FT method.

Keywords: pitch evaluation, cross-correlation, pitch and uniformity measurement, SPM

1. Introduction

In nanometer metrology and measurement, one-dimensional (1D) nanostructures and gratings are crucial artifacts. When metrologically certified, they are broadly applied as the reference materials to pair with sub-nanometer resolution of atomic force microscope (AFM) cantilevers as an encoder[1,2], nanometer resolution of optical grating encoders[3-5], to calibrate scanning probe microscopes (SPM) [6] and to calibrate stylus profilers [7] etc. The pitches of a grating can be calibrated if a micro- or nano-probe has been integrated into a laser interferometer based measuring system as the standard instrument, such as metrological AFMs in world leading national metrology institutes [8-11]. The pitch evaluations are based on the centre-of-gravity (CG) [11-13] and Fourier-transform-based (FT) [13] methods. The pitches of the rectangular, isosceles trapezoidal structure gratings have been evaluated by calculating the CG because the grating structures have two obvious steep sides between one waveform and the adjacent waveform.

Owing to the surface contamination, surface defects from the fabrication and abrasion of the cantilever tip or a probe stylus etc., grating position-related topographical signals are always accompanied by noise. The noise makes the regular waveform of signals irregular, such as a probed topographical signal shown in figure 1. It is very difficult to practically apply the CG method to determinate the pitch parameter from the measured topographical signals with the noise and irregularities. The FT method is the most precise to find the fundamental frequency of a 1D grating position-related signal because the pitch is the reciprocal of the fundamental frequency. However, the FT method cannot give the information about the pitch uniformity which is another significant parameter to fabricate and calibrate 1D grating.

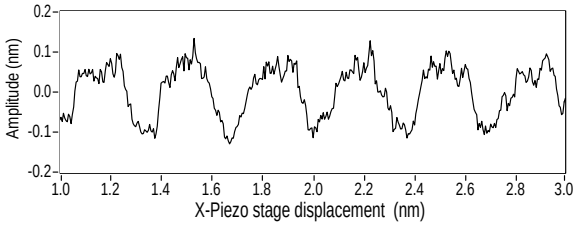

Figure 1. Grating position-related topographical signal with noise and irregular waveform measured by UHV STM.

To efficiently employ CG, FT or other pitch evaluation methods, it is very important to apply a digital filtering technique to filter the measured signal so as to obtain a good signal-to-noise ratio (SNR), and to get accurate integer period peak or valley positions.

In the previous investigation, real-time filtering of 1D sinusoidal grating position-encoded signal was performed [14]: a cross-correlation technique has been employed to filter a 1D grating position-encoded signal; a half sinusoidal waveform template was being proven to be very efficient and accurate to filter 1D sinusoidal grating-encoded signal by cross-correlating with it in real time. It is predicted that the cross-correlation filter, if applied for the pitch evaluation of the 1D arbitrarily structured grating, can achieve very similar accuracy to the FT method. In the following sections, after the mathematical explanation that the 1D sinusoidal grating position-related topographical signal with noise is filtered by a cross-correlation filter - a half sinusoidal waveform template, the mathematic equations are derived and the computer simulation is conducted to see to what extent that the cross-correlation filter can be effectively and precisely applied to filter 1D arbitrary-structured grating position-related topographical signal, and whether or not the evaluated pitches from the filtered signal can achieve the same pitch values as that the FT method does. Finally it is applied for the evaluation of two 1D grating position-related topographical signals that are scanned by a UHV STM and metrological AFM respectively.

2. 1D sinusoidal grating

2.1 1D grating position-related topographical signal

When a 1D grating is probed by a micro- or nano-probe along the direction crossing the grating lines, the plotted topographical signal y_n against the displacement x_n consists of many countable integer waveforms, noise and low frequency tilt signals shown in figure 1.

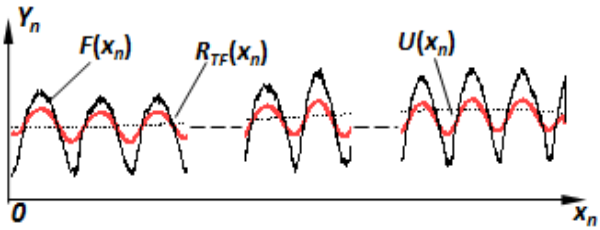

Figure 2. 1D sinusoidal grating position-related signal $F(x_n)$ probed by tuning-fork cantilever AFM. It consists of sinusoidal, noise and tilt drafting signals.

$F(x_n)$ represents 1D sinusoidal grating position-related signal plotted in the solid thin-line in figure 2. It is resolved into a sinusoidal signal $f(x_n)$, a white noise $W(x_n)$ and a low frequency tilt signal $U(x_n)$ (dotted-line in figure 2), which is

$$F(x_n) = f(x_n) + U(x_n) + W(x_n) \tag{1}$$

where, $F(x_n)$, $f(x_n)$, $U(x_n)$ and $W(x_n)$ are all finite discrete sequences with number *N* of data points at a scanning range, and

$$f(x_n) = A\sin\frac{2\pi x_n}{p}, \quad 0 \le n \le N-1 \tag{2}$$

where, p denotes the period of signal sequence $F(x_n)$.

The noise is directly presented by its absolute amplitude ***a***:

$$W(x_n) = a_n \qquad 0 \le n \le N-1 \tag{3}$$

$U(x_n)$, caused by the micro-moving stage or a tilted 1D grating, is expressed as a polynomial function:

$$U(x_n) = H_0 + H_1 \cdot x_n + \cdots + H_K \cdot x_n{}^K, \qquad 0 \le n \le N-1 \tag{4}$$

where, H_0, H_1, $\cdots, H_K$ are the constant item, coefficient of monomial item, coefficient of quadratic item, $\cdots$, and coefficient of K^{th} order item respectively.

2.2 Signal filtered by a cross-correlation filter

If a half sinusoidal waveform template $T(x_n)$ has *M* numbers of data and p_T numbers of period in the sequence, which satisfies the equation of $M = p_T / 2$,

$$T(x_m) = B\sin\frac{2\pi x_m}{p_T}, \quad 0 \le m \le M-1 \tag{5}$$

The cross correlation of $F(x_n)$ and $T(x_m)$ is

$$R_{TF}(x_n) = R_{Tf}(x_n) + R_{TU}(x_n) + R_{TW}(x_n) \tag{6}$$

where $R_{TF}(x_n)$, $R_{Tf}(x_n)$, $R_{TU}(x_n)$ and $R_{TW}(x_n)$ is the cross-correlation signal, cross-correlation sinusoidal signal, cross-correlation tilt signal and cross-correlation noise respectively, and $0 \le n < N+M-1$, which means in cross-correlation sequence total number is $(M+N)$, *M* is the number of elements in the sequence of $T(x_m)$, *N* is the number of elements in the sequence of $F(x_n)$.

$R_{TU}(x_n)$ still is a low frequency tilt drift signal, because

$$\begin{aligned} R_{TU}(x_n) &= \frac{B}{M}\sum_{m=0}^{M-1}\{\sin\frac{2\pi x_m}{p_T}\cdot[H_0 + H_1\cdot(x_m + x_n) + \cdots + H_K\cdot(x_m + x_n)^K]\} \\ &= J_0 + J_1\cdot x_n + J_2\cdot x_n{}^2 + \cdots + J_K\cdot x_n{}^K \end{aligned} \tag{7}$$

where, J_0, J_1, $J_2, \cdots, J_K$ are the constant item, coefficient of monomial item, coefficient of quadratic item, …, and coefficient of K^{th} order item respectively. According to binominal theorem, the coefficient of each item J_i $(i = 0,\ 1,\ 2,\ \cdots,\ K)$ in equation (7) is expressed as

$$\begin{cases} J_0 = B\sum_{m=0}^{M-1}[\sin\frac{2\pi x_m}{p_T}\cdot\sum_{i=0}^{K}\binom{i}{0}\cdot H_i\cdot x_m^i] \\ J_1 = B\sum_{m=0}^{M-1}[\sin\frac{2\pi x_m}{p_T}\cdot\sum_{i=1}^{K}\binom{i}{1}\cdot H_i\cdot x_m^{i-1}] \\ J_2 = B\sum_{m=0}^{M-1}[\sin\frac{2\pi x_m}{p_T}\cdot\sum_{i=2}^{K}\binom{i}{2}\cdot H_i\cdot x_m^{i-2}] \\ \cdots\cdots \\ J_K = B\sum_{m=0}^{M-1}[\sin\frac{2\pi x_m}{p_T}\cdot\sum_{i=K}^{K}\binom{i}{K}\cdot H_i\cdot x_m^{i-K}] \end{cases} \quad (8)$$

where, $\binom{i}{j} = \frac{i!}{j!(i-j)!}$ and $i \geq j$.

The cross-correlation signal is

$$R_{Tf}(x_n) = \frac{1}{M}\sum_{m=0}^{M-1}T(x_m)\cdot f(x_m+x_n) = \frac{AB}{M}\sum_{m=0}^{M-1}\sin\frac{2\pi x_m}{p_T}\cdot\sin\frac{2\pi(x_m+x_n)}{p}$$
$$= C_1[M, p_T]\cdot\cos\frac{2\pi x_n}{p} + C_2[M, p_T]\cdot\sin\frac{2\pi x_n}{p} = C[M, p_T]\cdot\sin(\frac{2\pi x_n}{p} + \phi[M, p_T]) \quad (9)$$

where, $C_1[M, p_T] = \frac{AB}{M}\sum_{m=0}^{M-1}\sin\frac{2\pi x_m}{p_T}\cdot\sin\frac{2\pi x_m}{p}$, $C_2[M, p_T] = \frac{AB}{M}\sum_{m=0}^{M-1}\sin\frac{2\pi x_m}{p_T}\cdot\cos\frac{2\pi x_m}{p}$,

$\phi[M, p_T] = \tan^{-1}(C_2[M, p_T]/C_1[M, p_T])$ and $C[M, p_T] = (C_1^2[M, p_T] + C_2^2[M, p_T])^{1/2}$.

From equation (9), it is seen that $R_{Tf}(x_n)$ remains sinusoidal signal sequence. It has period p which is the same as $f(x_n)$, although the amplitude changes to $C[N, p_T]$ and the phase has a shift of $\phi[M, p_T]$. Since $R_{TU}(x_n)$ is a low frequency tilt signal, it cannot modulate the period of $R_{TF}(x_n)$, and it can be easily corrected using mathematic method. Therefore, equation (6) becomes

$$R_{TF}(x_n) = R_{Tf}(x_n) + R_{TW}(x_n) = C[M, p_T]\cdot\sin(\frac{2\pi x_n}{p} + \phi[M, p_T]) + R_{TW}(x_n) \quad (10)$$

The cross-correlation noise in equation (10) is expressed as

$$R_{TW}(x_n) = \frac{1}{M}\sum_{m=0}^{M-1}T(x_m)\cdot W(x_m+x_n) = \frac{B}{M}\sum_{m=0}^{M-1}a_{m+n}\cdot\sin\frac{2\pi x_m}{p_T} \quad (11)$$

If $\bar{A_m} = \frac{B}{M}\sin\frac{2\pi x_m}{p_T}$ is set, equation (11) is rewritten as

$$R_{TW}(x_n) = \sum_{m=0}^{M-1}\bar{A_m}\cdot a_{m+n} \quad (12)$$

It is actually the operation of weighted moving average (WMA) of the noise signal by using a set of data $\bar{A_m}$ $(0 \leq m \leq M-1)$ as the weights. Therefore, after the cross-correlation filtering, the noise signal series a_n $(0 \leq n \leq N-1)$ with highly dense irregularities becomes a slow changing noise series $R_{TW}(x_n)$. It is estimated that the slow changing $R_{TW}(x_n)$ does not influence the period but can more or less modulate the amplitude of the cross-correlation sinusoidal signal $R_{Tf}(x_n)$ in equation (10). An example below demonstrates the influence of the noise on the sinusoidal signal before and after cross-correlation filtering.

a) If a series of 1000 Bernoulli noise data $W(n)$ with amplitude of 1 arbitrary unit in 50% probability , plotted in thin line in figure 3(a), is cross-correlated with a half sinusoidal waveform template $T(m)$ with 25 samples (M = 25 and p_T = 50) and 1 arbitrary unit amplitude, the normalized cross-

correlation noise $R_{TW}(x_n)$ which is plotted in thick-line in figure 3 (a) exhibits the slow changing random waveforms;

b) if a series of 1000 sinusoidal signal data $f(n)$with amplitude of 1 arbitrary unit and period of 50 (p = 50) data points is cross-correlated with $T(m)$, the cross-correlation signal $R_{Tf}(n)$, plotted in dash-line in figure 3 (b), is a series of sinusoidal waveform signal with the same period p; if $f(n)$ is mixed with the noise $W(n)$, the mixed signal $F(n)$ shown in figure 3 (c) is formed. It is less possible to evaluate the pitches from $F(n)$ by using other methods than the FT method. However, pitches can be evaluated from the cross-correlation signal $R_{TF}(n)$ shown in figure 3 (b) by detecting the peak positions in the horizontal axis, although it is modulated more or less by $R_{TW}(n)$ shown in figure 3(a).

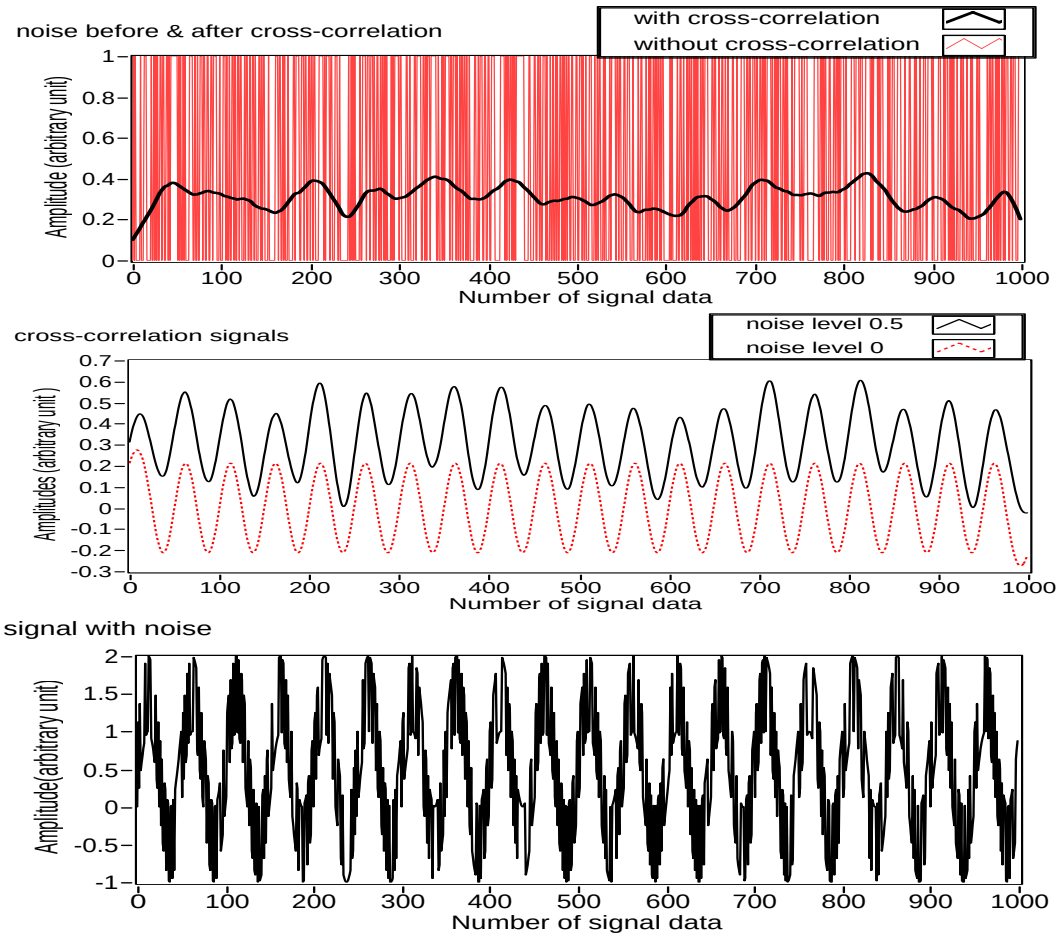

Figure 3. Influence of Bernoulli noise on sinusoidal signal before and after cross-correlation filtering (a) Bernoulli noise before and after cross-correlation filtering; (b) cross-correlation signals before and after mixed with Bernoulli noise and (c) sinusoidal signal influence by Bernoulli noise.

The previous simulations and experiments [14] have described and proven that if a half sinusoidal waveform template with sample $M = p_T / 2$ is taken as a filter,

a) if p_T is chosen any number in a small mathematic interval including or closer to p, especially $p_T \approx p$, the amplitude $C[M, p_T]$ will reach its maximum, the noise can be mostly suppressed;

b) if $p_T << p$, the number in the set of weights is relatively not enough to average the noise so that cannot be totally suppressed;

c) if $p_T >> p$, to a certain extent the amplitude of $R_{TF}(x_n)$ drops as small as $R_{TW}(x_n)$ so that signal to noise ratio (SNR) is too low to distinguish periodical signal from noise.

If the 1D simulated sinusoidal grating-related signal $F(x_n)$ has the pitch of p and amplitude of one arbitrary unit and is accompanied with noise of 0.3 arbitrary unit, the calculated $R_{TF}(x_n)$, $R_{TW}(x_n)$ and SNR plotted in figure 4 can explain the aforementioned conclusions best, when p_T is chosen to be the different multiple of a p.

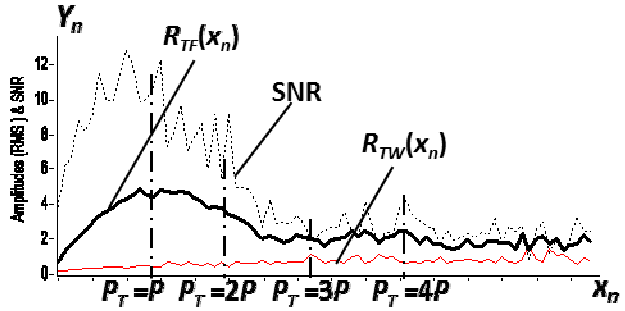

Figure 4. $R_{TF}(x_n)$, $R_{TW}(x_n)$ and SNR change with p_T

Therefore, instead of directly calculating the pitches from the original measured signal $F(x_n)$, the cross-correlation signal $R_{TF}(x_n)$ is validated to calculate the pitches when $p_T \approx p$. For 1D sinusoidal grating position-related signal $F(x_n)$ probed by an AFM in figure 2, the cross-correlation signal $R_{TF}(x_n)$ ($0 \le n < N-1$) is plotted in solid gross-line after the extra M number of data in the two ends of its sequence are cut-off from the series of data.

3. Pitch evaluation based on peak detection (PD)

After filtering, the low drifting tilt topographical signal $U(x_n)$ and its cross-correlation signal $R_{TW}(x_n)$ shown in figure 2 have been eliminated by using the mathematic method as shown in figure 5. If the coordinates of the peaks are detected as p_1, p_2, p_3,$\cdots$,p_L, along the probe-scanning direction ② (parallel to x-axis) which forms a small angle α relative to the direction ① perpendicular to the 1D grating lines (perpendicular direction) , as shown in figure 6 (a), the distance between any two adjacent waveform peaks in the noise-free cross-correlation signal in the perpendicular direction is one pitch value. The individual pitch is calculated by

$$\begin{cases} P_1 = (p_2 - p_1)\cdot\cos\alpha \\ P_2 = (p_3 - p_2)\cdot\cos\alpha \\ \cdots \\ P_{L-1} = (p_L - p_{L-1})\cdot\cos\alpha \end{cases} \tag{13}$$

The average of the pitches is

$$\bar{P} = \frac{1}{L-1}\sum_{i=1}^{L-1} P_i \tag{14}$$

The uniformity of the pitches is calculated by

$$\delta = \frac{1}{L-1}\sqrt{\sum_{i=1}^{L-1}(P_i - \bar{P})^2} \tag{15}$$

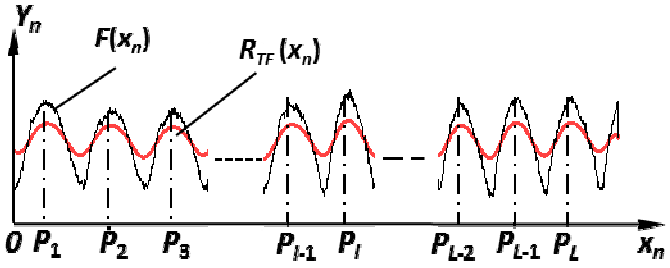

Figure 5. Signal $F(x_n)$ and $R_{TF}(x_n)$ after the low frequency tilt signal $U(x_n)$ and $R_{TU}(x_n)$ are eliminated in figure 2.

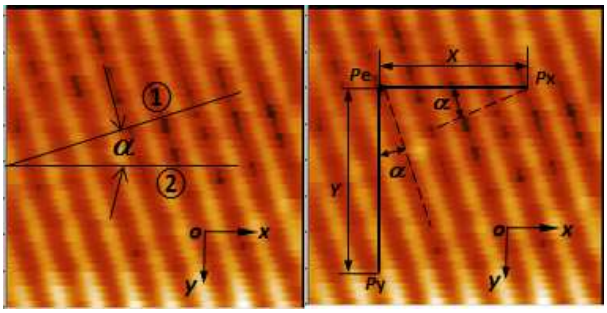

(a) (b)

Figure 6. A tilt angle α between perpendicular direction ① and probe-scanning direction ② is shown in (a) and the diagram on evaluation of tilt angle α is shown in (b).

The PD method is also used to decide the tilt angle α [15,16], as shown in figure 6 (b) . If the stylus scans the 1D grating firstly by a displacement X from P_e to P_x and then returns to P_e, and secondly by a displacement Y from P_e to P_y and returns to P_e too, X and Y can be expressed respectively as

$$\begin{cases} X = (fsx + Ix + fex) \cdot p / \sin\alpha \\ Y = (fsy + Iy + fey) \cdot p / \cos\alpha \end{cases} \tag{16}$$

Therefore

$$\alpha = \arctan(\frac{Y}{X} \cdot \frac{Ix + fsx + fex}{Iy + fsy + fey}) \tag{17}$$

where, *Ix*, *fsx* and *fex* are the counted integer periods, calculated fractional parts at the beginning and the end of the signal in *x* direction respectively; *Iy*, *fsy* and *fey* are the counted integer periods, calculated fractional parts at the beginning and the end of the signal in *y* direction respectively.

4. 1D arbitrarily structured grating

For a 1D, *p*-periodic and arbitrarily structured grating position-related signal, if in the interval $[-\frac{p}{2}, \frac{p}{2})$ it is mathematically expressed as

$$f(x_n) = \begin{cases} -f(-x_n), & \frac{p}{2} \le x_n < 0 \\ f(x_n), & 0 \le x_n < \frac{p}{2} \end{cases} \tag{18}$$

It can be expressed by a Fourier sine series

$$f(x_n)=\sum_{k=1}^{\infty}A_k\cdot\sin\frac{2k\pi x_n}{p}\qquad(0\le n\le N-1)\tag{19}$$

where, $A_k=\frac{4}{p}\int_0^{p/2}f(x_n)\cdot\sin\frac{2k\pi x_n}{p}dx_n,(k=1,2,3,\cdots)$.

If it is cross-correlated with a half waveform of sinusoidal template with the same period *p*, i.e.,

$$T(x_m)=B\sin\frac{2\pi x_m}{p}\qquad(0\le m<M-1)\tag{20}$$

$$\begin{aligned}R_{Tf}(x_m)&=\frac{B}{M}\sum_{m=0}^{N-1}T(x_m)\cdot f(x_m+x_n)\\&=\frac{B}{M}\sum_{m=0}^{M-1}\sin\frac{2\pi x_m}{p}\cdot[A_1\sin\frac{2\pi(x_m+x_n)}{p}+A_2\sin\frac{4\pi(x_m+x_n)}{p}+\cdots+A_k\sin\frac{2k\pi(x_m+x_n)}{p}+\cdots]\end{aligned}\tag{21}$$

Since the ***k***th item in equation (21) can be factorized as

$$\begin{aligned}&\sum_{m=0}^{M-1}\sin\frac{2\pi x_m}{p}\cdot A_k\sin\frac{2\pi(x_m+x_n)}{p_k}\\&=A_k\sum_{m=0}^{M-1}[\sin\frac{2\pi x_m}{p}\cdot\sin\frac{2k\pi x_m}{p}]\cdot\cos\frac{2k\pi x_n}{p}+A_k\sum_{m=0}^{M-1}[\sin\frac{2\pi x_m}{p}\cdot\cos\frac{2k\pi x_m}{p}]\cdot\sin\frac{2k\pi x_n}{p}\\&=C_1[M,k]\cdot\cos\frac{2k\pi x_n}{p}+C_2[M,k]\cdot\sin\frac{2k\pi x_n}{p}\\&=C[M,k]\cdot\sin(\frac{2k\pi x_n}{p}+\phi[M,k])\end{aligned}\tag{22}$$

where, $C_1[M,k]=\frac{A_kB}{M}\sum_{m=0}^{M-1}\sin\frac{2\pi x_m}{p}\cdot\sin\frac{2k\pi x_m}{p}$, $C_2[M,k]=\frac{A_kB}{M}\sum_{m=0}^{M-1}\sin\frac{2\pi x_m}{p}\cdot\cos\frac{2k\pi x_m}{p}$,

$C[M,k]=(C_1^2[M,k]+C_2^2[M,k])^{1/2}$, $\phi[N,k]=\tan^{-1}[C_2[N,k]/C_1[N,k]]$ and $(k=1,2,3,\cdots)$.

The equation (21) becomes

$$R_{Tf}(x_n)=C[M,1]\cdot\sin(\frac{2\pi x_n}{p}+\phi_1)+C[M,2]\cdot\sin(\frac{4\pi x_n}{p}+\phi_2)+\cdots+C[M,k]\cdot\sin(\frac{2k\pi x_n}{p}+\phi_k)+\cdots\tag{23}$$

Equivalently, it is written as

$$R_{Tf}(x_n)=C[M,1]\cdot\sin(\frac{2\pi x_n}{p}+\phi_1)+C[M,2]\cdot\sin(\frac{2\pi x_n}{p_2}+\phi_2)+\cdots+C[M,k]\cdot\sin(\frac{2\pi x_n}{p_k}+\phi_k)+\cdots\tag{24}$$

where, $p_k=p/k$, $(k=2,3,4,\cdots)$.

To examine equation (24), it is found that for a 1D, *p*-periodic and arbitrarily structured grating position-related topographical signal, when cross-correlated with a half sinusoidal waveform template of *p*-period, the cross-correlation signal consists of fundamental period and 2, 3, 4,$\cdots k,\cdots$ harmonic sinusoidal waveforms. Since $|A_k|$ decreases greatly with *k* increasing according to the training of representing an arbitrary function by a Fourier series, it is predicated that $|C[M,k]|$ decreases steeply with *k* increasing and sinusoidal waveform in fundamental period (the first item) dominates in equation (24).

Taking 1D rectangular grating and 1D triangular grating as two examples, their mathematic expressions are respectively

$$f_r(x_n)=\begin{cases}-h, & -p/2\le x_n<0\\ h, & 0\le x_n<p/2\end{cases}\qquad(h\ne0)\tag{25}$$

and

$$f_t(x_n)=\begin{cases}\dfrac{sx_n}{2}, & 0\le x_n<\dfrac{p}{4}\\ \dfrac{s(0.5p-x_n)}{2}, & \dfrac{p}{4}\le x_n\le\dfrac{p}{2}\end{cases} \tag{26}$$

They can be represented as *I*-harmonic Fourier sine series which are respectively

$$f_r(x_n)=\frac{4h}{\pi}\sum_{k=1}^{I}\frac{1}{2k-1}\sin\frac{2(2k-1)\pi x_n}{p} \tag{27}$$

and

$$f_t(x_n)=\frac{sp}{\pi^2}\sum_{k=1}^{I}\frac{(-1)^{k-1}}{(2k-1)^2}\sin\frac{2(2k-1)\pi x_n}{p} \tag{28}$$

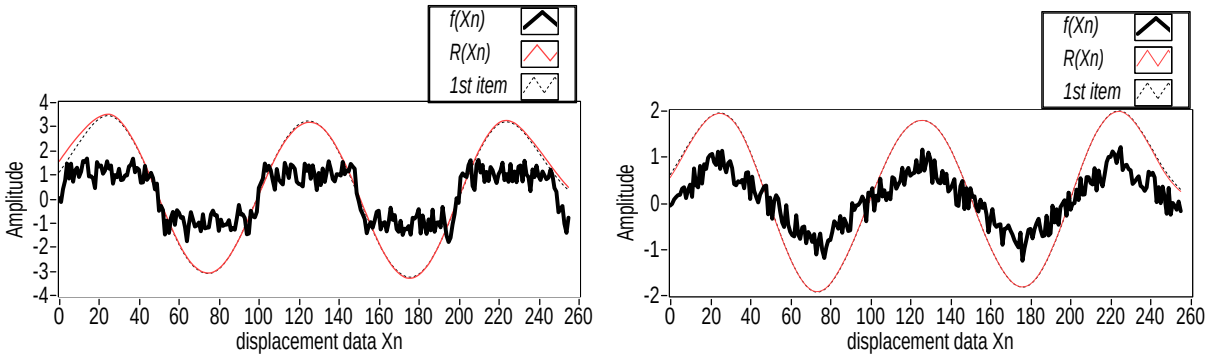

(a) (b)

Figure 7. Simulations of 1D rectangular grating and 1D triangular grating position- related signals in legend $f(Xn)$ and their cross-correlation signals in legend $R(Xn)$ are shown in (a) and (b) respectively.

With pitch p=100 arbitrary units, 256 displacement data, 1 arbitrary unit in amplitude which means h=1 in equation (25) and s=8/p in equation (26), and noise of 0.5 arbitrary unit in amplitude, 5-harmonic (I=5) Fourier series approximation of 1D rectangular grating and 1D triangular grating topographical signals are plotted in thick solid-line with the legend-$f(Xn)$ in figure 7 (a) and (b) respectively. The cross-correlation signals of the sum of 5 items with the legend-$R(Xn)$ and the fundamental period item with the legend-1*st item* are also plotted in thin solid-line and thin dash-line in figure 7 (a) and (b) respectively.

5. Experiments and results

5.1 Comparison of PD with FT

In order to see how pitch evaluated by the PD method is in agreement with that evaluated by the FT method and how pitch evaluated by both PD and FT are in agreement with true pitch value, the simulation is conducted by using LabVIEW™. When the noise presents in different distribution patterns, first 1D sinusoidal, 1D rectangular and 1D triangular gratings with 100 (p=100) and 1 arbitrary unit in pitch and amplitude and 1000 simulated data, are evaluated in pitch by using the FT method, then they are cross-correlated by a half sinusoidal waveform with 100 (p_T =100) and 1 arbitrary units in period and amplitude. After that, the pitches are evaluated by using PD method. The simulation is repeated 100 times at each noise level, the average of pitch deviations (APD) from the true pitch value, i.e. 100 arbitrary units, is calculated each time. Since the randomly generated noise signal varies a little from one time to the others, so does the pitch deviation. Therefore, the APD and the corresponding variations – represented by standard deviation (STD) are calculated.

The noise signals in uniform white, Gaussian white, binomial and Bernoulli distributions which possibly exist

in 1D grating topographical signals probed by scanning probe microscopes (SPMs) are tested. When the amplitude of uniform white noise, standard deviation of Gaussian white noise, trail probability of binomial noise and ones probability of Bernoulli increases from 0.1 to 0.5, the simulation results are listed in table 1, where the APD and STD data that are larger than 0.5 data point are highlighted in bold font. For each noise distribution pattern, both APD and STD are zero if the noise level is zero, and the pitch deviation and variation increase more or less with the noise level increasing by using both FT and PD method. It is concluded from table 1,

(1) for the uniform white noise, both APD and STD are within 0.20 % in PD and FT, which means the measured pitches in PD and FT method are both 99.8% in agreement to the true pitch value;

(2) for the Gaussian white, binomial and Bernoulli noise that coexists with sinusoidal and rectangular waveform signals, it is seen that in maximum the 0.07% APD in PD method is smaller than 0.23% in FT method. However, 0.92% STD in PD method is larger than 0.25% in FT method. For the Gaussian white, binomial and Bernoulli noise that coexists with triangular waveform signal respectively, the maximum 0.60% APD in PD method is close to 0.48% in FT method. However, 2.54% STD in PD method is much larger than 0.28% in FT method.

Table 1 Simulation results of average pitch deviations (APD) and corresponding variations (STD) (unit: %)

Pitch evaluation method			**PD**					**FT**				
Noise (arbitrary units)			0.1	0.2	0.3	0.4	0.5	0.1	0.2	0.3	0.4	0.5
Uniform white	sinusoidal	APD	-0.01	-0.01	0.00	-0.01	-0.01	0.00	-0.01	0.20	-0.14	-0.14
		STD	0.11	0.10	0.10	0.10	0.11	0.12	0.10	0.10	0.11	0.11
	rectangular	APD	0.01	0.01	0.01	0.02	0.02	-0.01	0.06	0.05	-0.02	-0.03
		STD	0.03	0.04	0.06	0.08	0.09	0.02	004	0.05	0.07	0.09
	triangular	APD	-001	0.00	0.00	0.00	0.00	0.03	-0.09	-0.05	0.18	0.05
		STD	0.03	0.06	0.08	0.09	0.11	0.04	0.07	0.09	0.11	0.13
Gaussian white	sinusoidal	APD	0.00	0.00	0.00	0.00	-0.03	-0.04	0.11	0.04	0.01	0.18
		STD	0.05	0.08	0.10	0.13	0.49	0.05	0.09	0.13	0.16	0.19
	rectangular	APD	0.01	0.00	0.02	0.03	0.05	-0.02	0.15	0.08	-0.14	-0.02
		STD	0.05	0.08	0.10	0.13	0.24	0.05	0.07	0.09	0.11	0.20
	triangular	APD	-0.45	-0.43	-0.33	-0.22	-0.32	0.00	0.06	-0.15	-0.48	-0.02
		STD	**2.32**	**2.38**	**2.34**	**2.32**	**2.37**	0.28	0.28	0.28	0.28	0.28
binomial	sinusoidal	APD	0.01	-0.07	-0.07	-0.07	-0.06	0.15	-0.13	-0.12	-0.16	-0.02
		STD	0.14	**0.92**	**0.86**	**0.81**	**0.77**	0.19	0.21	0.22	0.24	0.25
	rectangular	APD	0.03	0.03	0.03	0.03	0.02	0.06	0.21	0.06	-0.07	-0.04
		STD	0.14	0.16	0.17	0.18	0.18	0.13	0.15	0.16	0.18	0.18
	triangular	APD	-0.40	**-0.53**	**-0.54**	**-0.51**	**-0.50**	-0.12	0.08	-0.18	-0.20	0.09
		STD	**1.99**	**2.26**	**2.28**	**2.22**	**2.14**	023	0.22	0.23	0.25	0.28
Bernoulli	sinusoidal	APD	0.02	-0.06	-0.06	-0.04	-0.03	-0.21	-0.03	-0.23	-0.04	-0.17
		STD	0.16	**0.84**	**0.85**	**0.74**	**0.67**	0.18	0.21	0.22	0.23	0.24
	rectangular	APD	0.03	0.03	0.01	0.01	0.01	-0.22	008	-0.05	-0.08	0.13
		STD	0.16	0.17	0.18	0.19	0.19	0.12	0.14	0.17	0.19	0.19
	triangular	APD	-0.28	-0.47	**-0.60**	**-0.53**	**-0.56**	0.12	-0.47	0.36	0.02	0.05
		STD	**1.70**	**2.27**	**2.54**	**2.40**	**2.41**	0.21	0.22	026	0.26	028

It is certain that both APD and STD in the FT method change less with the noise increasing or decreasing, no matter how the noise distributes. It is estimated, besides signal noise and time clock accuracy to generate the signal, the main factor that influences the accuracy of pitch evaluation in the FT method is the pitch calculation algorithm, as the pitch is the reciprocal of the fundamental frequency measured by using the Fourier transformation. Taking sinusoidal signal with nominal fundamental frequency of 0.01Hz as an example, although the measured frequency at the noise level of 0.5 arbitrary units is as accurate as 0.0100345 (0.345×10^{-4} Hz absolute deviation) , the calculated pitch of 99.659 data points (absolute deviation of 0.341data points) seems larger. Actually, the 0.345% and 0.341% relative deviations of the frequency and pitch are nearly equal.

It has been analyzed in section 2.1 that the main factor that influences the accuracy of pitch evaluation in the PD method is the noise level and noise distribution pattern, because the cross-correlation signal is the sum of the cross-correlation signal, although the latter is much smaller than the former. Since the average pitch deviation (APD) and pitch variation (STD) evaluated from triangular waveform with 0.5 arbitrary unit noise levels are generally less accurate than those from the other signals with noise. The cross-correlation signals with the noise in uniform white, Gaussian white, binomial and Bernoulli distributions of 0.5 arbitrary units in amplitude or 50% in ones probability are plotted together in figure 8. The differences of the horizontal peak positions between the four cross-correlation signals can be apparently distinguished.

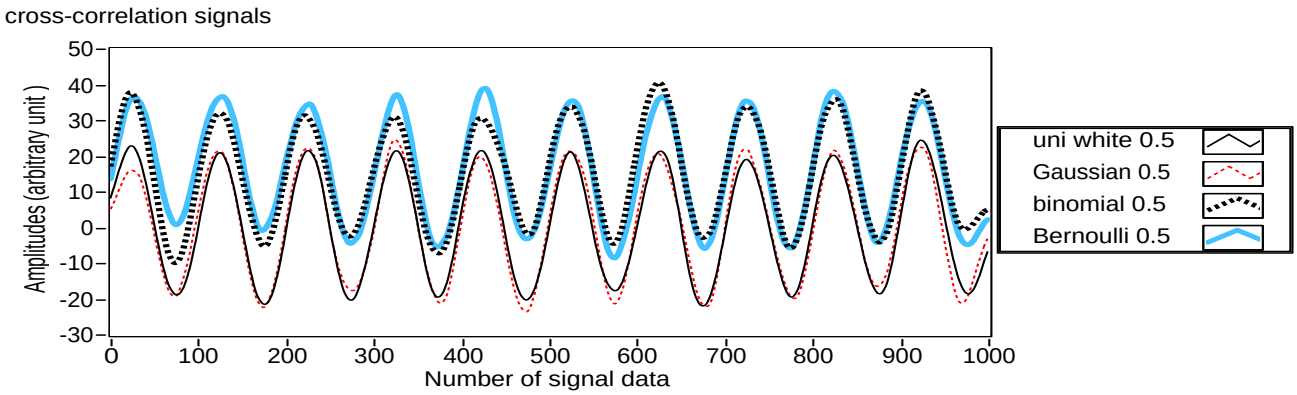

Figure 8. Cross-correlation triangular signals with noise of 0.5 arbitrary units in amplitude or 50% in ones probability.

5.2 Cross-correlation filtering and pitch evaluation in PD method

Two specimens, a highly oriented pyrolytic graphite (HOPG) with layer distance of 0.335 nm and a 1D pitch standard with nominal pitch of 3000 nm and standard deviation 20 nm, are measured by an ultra-high vacuum scanning tunneling microscope (UHV STM) and a metrological atomic force microscope (AFM) with 45° and 0° tilt angle angle, respectively. The data interval is 0.005 nm for STM and 2 nm for AFM; the acquired position and topographical data are 2 000 for STM and 20 000 for AFM. Two position-related topographical signals probed by UHV STM and metrological AFM respectively, with different noise levels and possible different noise distributions, are plotted in figure 9 (a) and (b). Since a half sinusoidal waveform template period p_T can be chosen equal to either the pitch value evaluated by the FT method or the data points roughly calculated from any period of topographical signal, the periods p_T of a half sinusoidal waveform template are approximately 80 data points for STM and 3000 data points for AFM, or the samples M ($M = 1/2p_T$) of a half sinusoidal waveform template are 40 for STM and 1500 for AFM respectively. The cross-correlation signals are plotted together with their topographical signals. The measured average pitch $\overline{P}$ in PD and FT method, the pitch uniformity δ in PD method are listed in table 2.

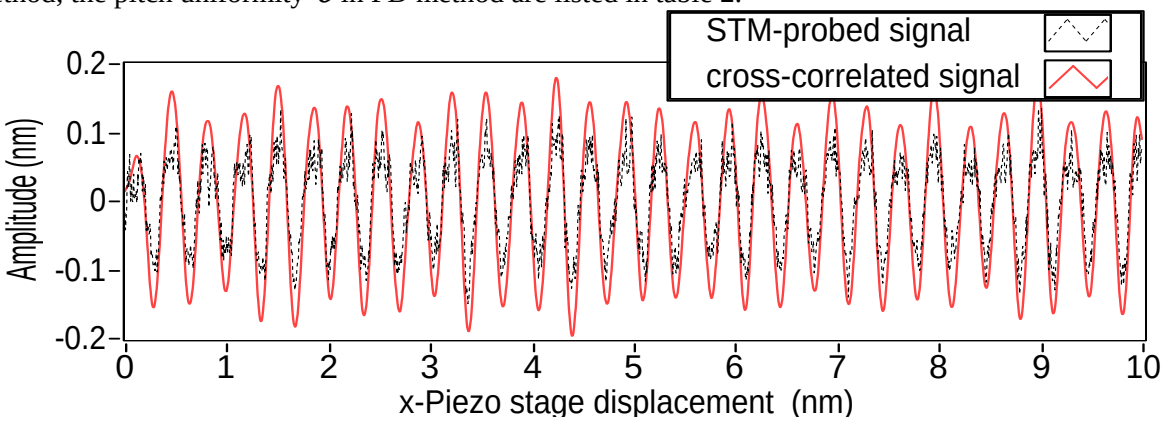

(a)

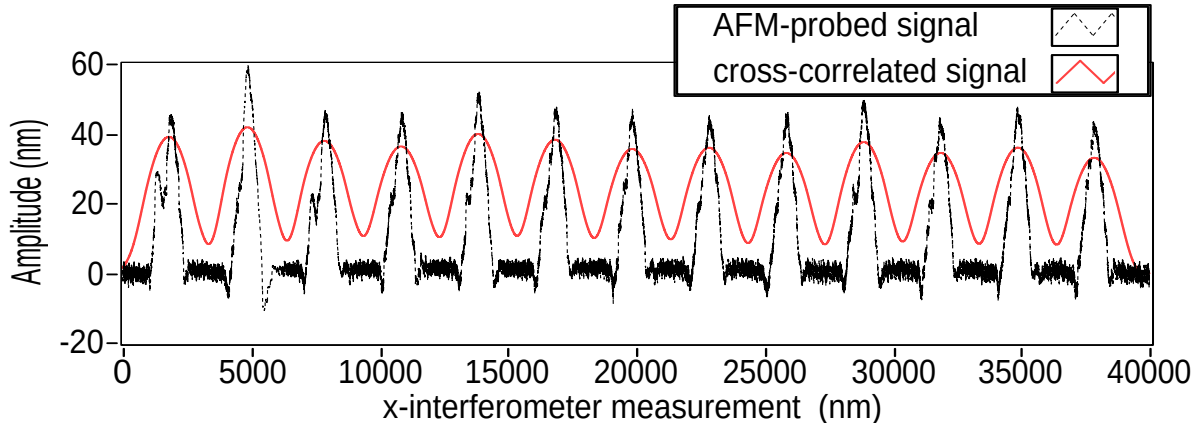

(b)

Figure 9. STM- and AFM-probed 1D grating position-related signals and their cross-correlation signals are plotted in (a) and (b) respectively.

Table 2 Average pitch $\bar{P}$ and uniformity δ

specimen	Nominal (nm)	PD (nm)		FT (nm)	
	P	$\bar{P}$	δ	$\bar{P}$	δ
HOPG	0.246	0.240	0.0142	0.240	-
grating	3000	3004.11	19.45	3003.34	-

5.3 Tilt angle measurement

Three different in-plane tilt angles of 1D sinusoidal grating of 300 nm in pitch are imaged in figure 10 (a), (b) and (c) respectively, which are denoted as in-plane angle I, II and III. If the *X* and *Y* displacements of the *x-y* piezoelectric micro-moving stages are preset 3000, 2000 and 3000 moving steps for I, II and III respectively in closed-loop control by the built-in capacitance sensors with non-linearity less than 0.1%, the 10 times of angle measurements results, average and standard deviation (STD) are listed in table 3.

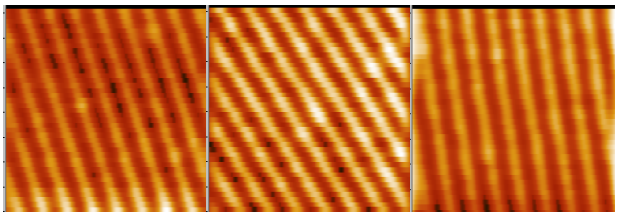

(a) (b) (c)

Figure 10. (a), (b) and (c) are the images of 1D sinusoidal grating with in-plane orientation angle I, II and III respectively.

Table 3. In-plane angle measurement results of 10 times corresponding to figure 10.

angle	Angle measurement results (°)					Average (°)	STD (°)
I	21.5601	21.5733	21.5690	21.5441	21.5467	21,5688	0,0267
	21.5434	21.5483	21.5741	21.6145	21.6140		
II	35.1994	35.1158	35.0793	35.0842	35.1194	35,1152	0,0387
	35.1321	35.0903	35.0649	35.1325	35.1343		
III	12.0863	12.0726	12.0552	12.0106	12.0054	12,0320	0,0565
	12.0529	12.0751	12.0842	11.9395	11.9380		

6. Conclusion

A half sinusoidal waveform template can be used as a cross-correlation filter in combination with cross-correlation technique. When a 1D arbitrarily structured grating position-related topographical signal, probed

by a micro- and nano-probe, is cross-correlated with it, and if its period p_T is approximately equal to that of 1D grating position-related signal, the noise can be very effectively filtered. After cross-correlation filtering, the peak positions can be detected from the cross-correlated topographical signal – denoted as the peak detection (PD) method, as the distance between any two adjacent waveform peaks along the direction perpendicular to 1D grating lines is one pitch value. It has been verified that the cross-correlation filter, if applied for the pitch evaluation of the 1D arbitrarily structured grating, can achieve the similar accuracy as the Fourier transformation based (FT) method. Cross-correlation filtering allows convenient, accurate and reliable evaluation of the local individual pitch, average and uniformity. Based on the cross-correlation filtering and the PD method, instead of intensity image scanning, the tilt angle between the perpendicular direction of 1D grating lines and the stylus-scanning direction can also be easily and quickly measured by the procedure introduced and described in this paper. It is an additional benefit to the precise pitch calculation and evaluation.

Acknowledgements

The authors gratefully acknowledge the UK's Engineering and Physical Sciences Research Council (EPSRC) funding of the EPSRC Centre for Innovative Manufacturing in Advanced Metrology (Grant Ref: EP/I033424/1) and Physiclisch-Technische Bundesanstalt (PTB) for the financial support to the PhD work of the authors.

References

[1] Chen X, Wolff H and Koenders L **2012** Atomic force microscope (AFM) cantilevers as encoder for real-time displacement measurements"*Proceedings of SPIE*. **8378** 923005 .
[2] Chen X, Koenders L, Wolff H, Neddermeyer H and Haertig F **2011** Atomic force microscope cantilevers as encoder for real time forward and backward displacement measurements, Meas. Sci. Technol. 22, 094017.
[3] Li J and Feldman M **2010** A prototype optical encoder system with nanometer measurement capability *Journal of Modern Optics*, **57** 1150 – 1156.
[4] Hsieh H, Lee J, Wu W, Chen J, Deturche R and Lerondel G **2010** Quasi-common-optical-path heterodyne grating interferometer for displacement measurement, *Meas. Sci. Technol*. **21** 115304.
[5] Lee J, Chen H, Hsu C and Wu C 2007 Optical heterodyne grating interferometry for displacement measurement with subnanometric resolution**,** *Sensors and Actuators A: physical*, **l 137** 185-191**.**
[6] ISO/DIS 11952 Surface chemical analysis — Scanning probe microscopy —Determination of geometric quantities using SPM: Calibration of measuring systems, *International Organization for Standardization*, 2011.
[7] ISO 5436-1 Geometrical Product Specifications (GPS) —Surface texture: Profile method; Measurement standards —Part 1: Material measures. *International Organization for Standardization*, 2001.
[8] Dai G, Pohlenz F, Danzebrink H-U, Xu M, Hasche K, and Wilkening G **2004** Metrological large range scanning probe microscope, *Rev. Sci. Instrum*. **75** 962-9.
[9] Kramar JA, Dixson R and Orji NG **2011** Scanning probe microscope dimensional metrology at NIST, *Meas. Sci. Technol*. **22** 024001.
[10] Leach R, Claverley J, Giusca C, Jones C, Nimishakavi L, Sun W, Tedaldi M and Yacoot A **2012** Advances in engineering nanometrology at the national physical laboratory, Meas. Sci. Technol. **23** 074002.
[11] Meli F and Thalmann R 1998 Long-range AFM profiler used for accurate pitch measurements *Meas. Sci. Technol.* **9** 1087-92.
[12] Misumi I, Gonda S, Kurosawa T and Takamasu K **2003** Uncertainty in pitch measurements of one-dimensional grating standards using a nanometrological atomic force microscope *Meas. Sci. Technol.* **14** 463-71.
[13] Dai G, Koenders L, Pohlenz F, Dziomba T and Danzebrink H-U **2005** Accurate and traceable calibration of one-dimensional grating *Meas. Sci. Technol.* **16**1241-49.
[14] Chen X, Koenders L and Haertig F **2011** Real-time cross-correlation filtering of a one-dimensional grating position-encoded signal *Meas. Sci. Technol.* **22** 085105.
[15] Boudreau B D and Raja J **1992** Analysis of lay characteristics of three-dimensional surface maps *Intern. J. Machine Tools and Manufacture* **32** 171-177.
[16] Chen X, Koenders L, Wolff H and Haertig F **2011** Tuning fork atomic force microscope cantilever encoder and applications for displacement and in-plane rotation angle measurement, ***Procedia Engineering***, vol. 25, pp. 555 – 558.